

Seed layer and multistack approaches to reduce leakage in SrTiO₃-based MIM capacitors using TiN bottom electrode

N. Menou¹, M. Popovici¹, K. Opsomer^{1,2}, B. Kaczer¹, M. A. Pawlak¹, A. Franquet¹, C. Detavernier², S. Van Elshocht¹, D. J. Wouters¹, S. Biesemans¹ and J. A. Kittl¹

¹IMEC, kapeldreef 75, B-3001 Leuven, Belgium

Phone: +32-16-28-10-69; E-mail: nicolas.menou@imec.be

²Ghent University, Krijgslaan 281/S1, B-9000 Ghent, Belgium

1. Introduction

Leakage reduction is crucial for MIM capacitors for future DRAM nodes. In previous investigations we showed that increasing the Sr-content would result in leakage reduction of SrTiO₃ (STO) films deposited on TiN [1]. In this work we demonstrate for thin (10nm) stoichiometric SrTiO₃ films that the leakage properties can be significantly lowered (while keeping high capacitance densities) by using stacking approaches such as seed layer (thin STO layer crystallized before the "bulk" STO deposition) and multistack STO/GdAlO₃/STO (Fig. 1).

2. Sample fabrication and physical analysis

SrTiO₃ layers were deposited by atomic layer deposition (ALD) in a cross-flow ASM Pulsar® 3000 reactor, at reactor temperatures of 250°C [2]. The precursors were Sr(t-Bu₃Cp)₂, H₂O, and Ti(OCH₃)₄ [2,3]. Stoichiometric STO films in the 10-20nm range were grown on TiN with good thickness and composition control over 300mm wafers [2]. Careful characterization of the SrTiO₃ crystallization behavior was achieved for the different stacks by in-situ XRD during ramp anneals in He (Fig. 2). At low temperature, SrTiO₃ peaks are observed only when a seed layer approach was used. This indicates that the seed was crystalline after anneal at 700°C in N₂ as confirmed in Fig.3a. The use of that crystalline seed helps to drastically lower the crystallization temperature of the "bulk" SrTiO₃ to ~420°C ($T_{\text{cryst}} \sim 520^\circ\text{C}$ for STO directly deposited on TiN) as shown on Fig.2 and Fig.3b. On the other hand, insertion of 1nm GdAlO₃ (deposited by ALD at 250°C) between two 7nm SrTiO₃ layers slightly increases the crystallization temperature of SrTiO₃. At high temperature, all films/stacks crystallized into the high-k perovskite SrTiO₃ phase. Those results imply two consequences regarding the crystallization anneal of the layers: (1) the low T_{cryst} obtained for the seed layer approach makes it possible to use crystallization anneals in O₂ even with TiN bottom electrodes. (2) Only N₂ anneals can be considered for crystallization of STO/GdAlO₃/STO stacks to avoid any damage (oxidation, roughening...) of the TiN bottom electrode. Nevertheless, considering the relatively high temperature (~600°C) required for crystallization of STO/GdAlO₃/STO stacks, one has to make sure that no major intermixing occurs between the constituting elements of the stack. Fig.4 shows time-of-flight secondary ion mass spectroscopy (TOF-SIMS) profiles of STO(15nm)/GdAlO₃(15nm)/Si stacks as deposited and after RTA at 600°C in N₂. The good overlap between both profiles indicates no significant intermixing between the two layers is induced by annealing. The slight shift of the Al signal into the SrTiO₃ layer after anneal would suggest a very limited (if any) diffusion of Al in SrTiO₃. The good stability of the STO/GdAlO₃ bilayer was confirmed by x-ray reflectometry (XRR) measurements

which show that the crystallization anneal has very little impact on the density of the GdAlO₃ layer (Tab.1). The higher density observed for SrTiO₃ is due to the crystallization.

3. Electrical evaluation

The electrical properties of the various stacks of interest (SrTiO₃ total thickness ~10nm) are presented in the following section. Based on the in-situ XRD results, SrTiO₃ films directly deposited on TiN (no seed) and STO/GdAlO₃/STO stacks were annealed at 600°C in N₂ while SrTiO₃ with seed approach were annealed at 450°C in O₂ (the seed anneal was done at 700°C in N₂). Pt top electrodes were deposited after crystallization anneal.

Fig.5 presents representative C-V curves measured on the stacks of interests. Relatively flat C-V characteristics with high capacitance densities (>35fF/cm²) are observed for 10nm films. The slightly lower capacitance obtained for stacking approach is compensated by a superior capacitance vs. voltage behavior. The capacitance and conductance dependence upon capacitor area are shown on Fig.6 for the studied stacks. Relatively high dielectric constants could be extracted from the linear slope C vs. size (K~66 for SrTiO₃ directly on TiN; K~51 for SrTiO₃ with seed layer; K~42 for STO/GdAlO₃/STO) and combined with low conductance. The influence of the stacking approaches on the leakage properties of 10nm SrTiO₃ based capacitors with TiN bottom electrode is depicted in Fig.7. Clearly, using a seed layer or a multistack approach leads to significant reduction in leakage; the IV curve being quite symmetric. J_g as low as 1.7×10⁻⁷ A/cm² (2.8×10⁻⁷ A/cm² and 6.2×10⁻⁷ A/cm²) were obtained at ±0.8V when using the seed layer (STO/GdAlO₃/STO multistack) approach.

4. Conclusion

Stacking approaches (*i.e.* seed layer and multistack STO/GdAlO₃/STO) were compared to standard deposition of stoichiometric SrTiO₃ directly on TiN. Optimized stacks are proven to be efficient for leakage reduction while keeping high dielectric performances even for thin layers (~10nm). The seed layer approach presents the advantage of lowering the crystallization T of the bulk SrTiO₃ making possible the use of O₂ crystallization anneal when using non-noble metal electrodes like TiN. This leads to excellent leakage densities (1.7×10⁻⁷ A/cm² at ±0.8V) and high capacitance properties (C_{density}~45fF/μm²). Such stacking approaches are of high interest in view of leakage reductions for next DRAM MIMCAP nodes.

References

- [1] N. Menou *et al.*, Tech. dig. IEDM. **2008**, 929.
- [2] M. Popovici *et al.*, submitted to J. Electrochem. Soc.
- [3] M. Vehkamäki, PhD Thesis, Univ. Helsinki (2007).

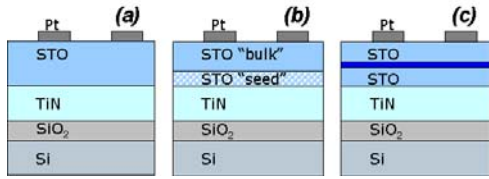


Fig. 1: Scheme of the studied SrTiO₃ based stacks. (a) STO deposited directly on TiN; (b) STO deposited on a seed layer (few nm) that is crystallized at 700°C in N₂; (c) Multistack STO/GdAlO₃/STO with GdAlO₃ thickness ~1nm

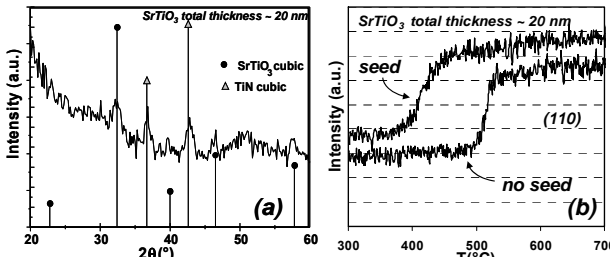


Fig. 3: (a) θ - 2θ scan of a 15nm SrTiO₃ film as deposited on a STO seed layer (~5nm) annealed at 700°C in N₂. The small STO peaks suggest that the seed layer is crystalline while the rest of the film is amorphous; (b) Intensity of the STO (110) peak as a function of T for STO films with and without seed layer measured by IS-XRD. Crystallization occurs at lower temperature when a seed layer is used.

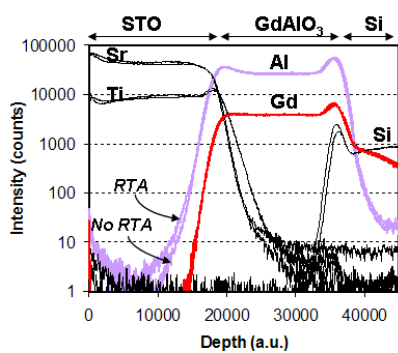


Fig. 4: TOF-SIMS profiles of STO/GdAlO₃/Si stacks as deposited and after RTA at 600°C in N₂. Overall no major change is observed. Only a slight shift of the Al signal into the STO layer after anneal would suggest a very small (if any) diffusion of Al in STO.

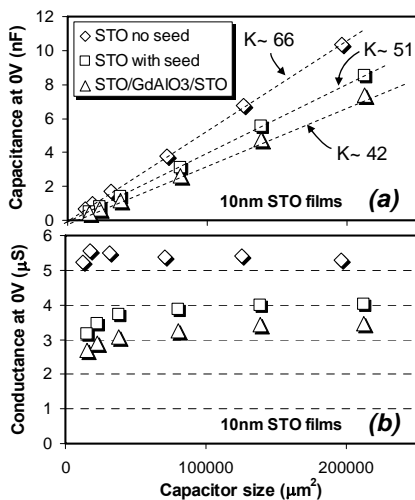


Fig. 6: C (a) and G (b) area scaling for crystalline 10nm SrTiO₃ stacks deposited on TiN (top electrode is Pt). K values of the different stacks are extracted from the slope C vs. size.

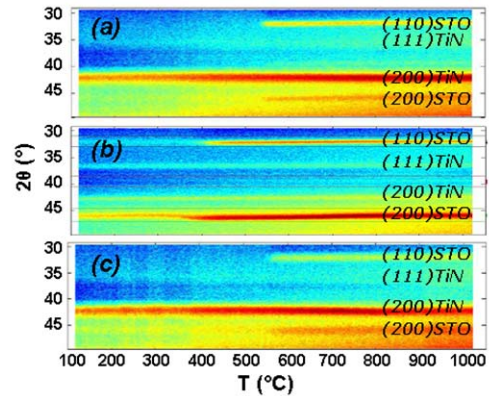


Fig. 2: In-situ XRD (0.2°C/s ramp, He) study of crystallization of thin ALD STO films (15-20 nm) on TiN. (a) SrTiO₃ deposited directly on TiN; (b) Seed layer approach; (c) STO/GdAlO₃/STO stacks. The temperature at which the STO layer crystallizes into the high-k perovskite structure depends on the stack.

	As deposited		After RTA 600°C	
	Thick. (nm)	Density(%)	Thick. (nm)	Density(%)
GdAlO ₃	15.4	70.0	14.1	71.6
SrTiO ₃	15.0	70.7	13.9	89.4

Tab. 1: Thicknesses and densities extracted from XRR measurements done on STO(15nm)/GdAlO₃(15nm)/Si stacks as deposited and after RTA at 600°C in N₂. No significant change is seen on the GdAlO₃ properties suggesting no intermixing with SrTiO₃.

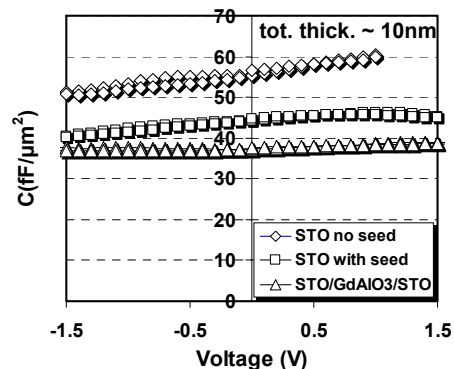


Fig. 5: C-V curves of crystalline 10nm SrTiO₃ stacks deposited on TiN (top electrode is Pt). Crystallization anneals were done by RTA for 60 sec.: at 600°C in N₂ for STO without seed and for STO/GdAlO₃/STO stacks; at 450°C in O₂ for STO with seed layer.

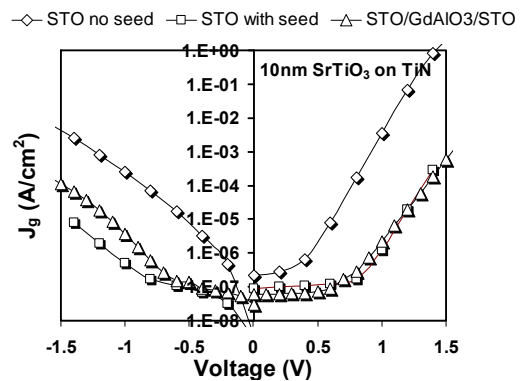


Fig. 7: I-V curves of crystalline 10nm SrTiO₃ stacks deposited on TiN (top electrode is Pt). The step delay time was 550ms. Strong leakage reduction is observed when using a stack approach (seed or multilayer).